Corrosion Inhibition of Aluminum in Hydrochloric Acid Solution Using Some Pyrazolocarbothioamide Derivatives

A. S. Fouda[1,], F.M. El-Taweel[2], M. Elgamil[1]*

[1] Department of Chemistry, Faculty of Science, El-Mansoura University, El-Mansoura-35516, Egypt,
[2] Department of Chemistry, Faculty of Science, Damietta University, Damietta, Egypt
[*]E-mail: asfouda@hotmail.com, asfouda@mans.edu.eg

The corrosion performance of Al in 2M HCl in presence of pyrazolocarbothioamide derivatives have been investigated using electrochemical frequency modulation (EFM), Tafel polarization (PP), AC impedance (EIS) and mass reduction (MR) techniques. From polarization studies, the adsorption of heterocyclic compounds retard liberation of hydrogen and decrease the metal dissolution i.e. they performance as mixed kind. The protection action of the (pyrazolocarbothioamide) was examined in view of the adsorbed of its parts on Al surface and follows kinetic-thermodynamic model isotherm. The inhibition efficiency (IE) increment as the pyrazolocarbothioamide derivatives concentration was increasing. The IE decreases with increasing the temperature, showing that it is physically adsorbed. It was revealed that the existence of these pyrazolocarbothioamide derivatives rise the energy of activation. Pyrazolocarbothioamide derivatives run as excellent coating film to Al versus corrosion in chloride containing solutions. Surface analysis was examined using atomic force microscopy (AFM) analysis. The obtained data from all investigated tests are in great agreement.

1. INTRODUCTION

Aluminum and its alloys speak to a vital arrangement of materials due to of their great advanced data and widespread variation of mechanical applications, predominantly in aviation, car and family unit enterprises. Al compounds appreciate an extensive variety of business use because of their various attractive properties, for example, astounding mechanical properties, high quality, low thickness, light weight, high warm conductivity. Be that as it may, responsive materials and are lying to corrosion [1]. Al/2Mg combination is utilized for tank warming loops in uninstalled petroleum bearers. HCl is generally utilized as a part of corrosive pickling, corrosive cleaning and oil well acidizing. Plus, acids increment rate of metal disintegration and are in charge of material

disappointment in a roundabout way. So, it is an importance to use a corrosion hindrance to lower metal dissolution. The greater part of understood corrosive inhibitors is hetero composite inclosing N, O and S [2-6]. The maximum significant problem in this part of investigation linked to Al protection versus corrosion. One of the greatest significant tests versus the corrosion is to utilized inhibitors. The greater part of inhibitor is to keep the Al from the aggressive medium or to adjust the reactions of electrode that basis of dissolution of the Al. The majority of the productive corrosive inhibitors are organic assembled that include for the best part S, N or O atom in their assembly. The IE of organic assembled is powerfully reliant on the building and chemical characteristic of the coating layer shaped on situations. Heterocyclic composite are outstanding for their efficacies as corrosion hindrance and those including N have been commonly discussed to in the works [7-8]. This is explaining by the presence Al atom that shape coordinative bonds with molecules ready to give electrons.

The motivation behind this work is to study the inhibition properties of investigated compounds and think about the corrosion hindrance value got from PP with that got by EIS, EFM studies and WR systems. The state of the external surface of the Al metal was contemplating by utilizing AFM. The temperature influence on the rate of corrosion and thermodynamic data were resolved and discussed.

2. MATERIALS AND TECHNIQUES

2.1. Solutions and materials

The working electrodes of Al in electrochemical tests were prepared from Al coins (99.98%)

2.2. Preparation of the inhibitors

Pyrazolocarbothioamide derivatives were set up in the research facility as indicated by the accompanying technique. Ethyl 3-thiosemicarbazido-butanoate was reacted with phenacyl bromide to achieve the ethyl 3-[(4-phenyl-2-thiazo-lyl) hydrazono] butanoate which experienced hetero cyclization by heating in ethanolic sodium acetic acid to obtain thiazolylpyrazolone that involved chemo selectively with perfumed aromatic diazonium salts to supply arylhy-drazonothiazolyl pyrazoles. Their action of pyrazolylthiosemicarbazones with phena-cylbromide gave the conforming 2-(arylidene-hydrazino) 4-phenylthiazoles in quantitative yields [9].

2.3. Chemicals and solutions

Working electrodes for electrochemical research were set up from Al coins. The aggressive solution utilized was set up by dissolution of analytical reagent 37% HCl with twice distilled water. 2 M HCl were set up by dissolution with twice-distilled water. 100 ml solutions (10^{-3} M) of each investigated compounds were set up by dissolution a precisely measured amount of every material in a 10 mL volume of dimethylformamide (DMF) and absolute ethanol. The required concentrations (5

$\text{x}10^{-6}$ - 21 $\text{x}10^{-6}$M) were set up by dilution with twice distilled water .The organic series inhibitors that utilized as a part of this study were recorded in Table1.

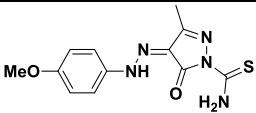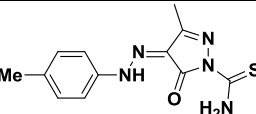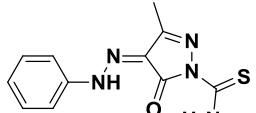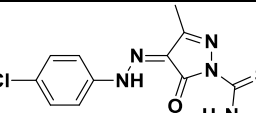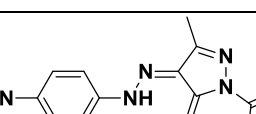## 2.4. Techniques utilized for corrosion tests

2.4.1. Weight reduction technique

The weight reduction (WR) tests were completed utilizing square specimens of size $2 \times 2 \times 0.2$ cm. The coins were first abraded to a mirror utilizing (400, 800 and 1500) coarseness emery paper, degreased in $(CH_3)_2CO$ lastly rinse with twice-distilled water, dried and then weighed. The coins were immersed in a 100 ml beaker set in water thermostat which containing 100 ml of 2 M HCl with and without various concentrations of examined pyrazolocarbothioamide derivatives. The inhibition efficiency (% IE) and the degree of surface coverage (θ) of pyrazolocarbothioamide derivatives for the corrosion of Al were computed as in eq. (1)

$$\% \text{ IE} = \theta \text{ x } 100 = 100 \times [(W^o - W) / W^o] \tag{1}$$

Where W^o and W are the values of the average weight losses without and with PYRAZOLOCARBOTHIOAMIDE DERIVATIVES, correspondingly.

Table 1. Chemical structures and characteristic of the examined pyrazolocarbothioamide derivatives

Compound	Structures	Names	Mol. Formulas, Mol. Weights
A		(E)-4-(2-(4-methoxy phenol) hydrazono)-3-methyl-5-oxo-4,5-dihydro-1H-pyrazole-1-carbothioamide	$C_{12}H_{13}N_5O_2S$ 291.08
B		(E)-3-methyl-5-oxo-4-(2-p-tolylhydrazono)-4,5-dihydro-1H-pyrazole-1-carbothioamide	$C_{12}H_{13}N_5OS$ 275.08
C		(E)-3-methyl-5-oxo-4-(2-(p-tolyl)hydrazono)-4,5-dihydro-1H-pyrazole-1-carbothioamide	$C_{11}H_{11}N_5OS$ 261.07
D		(E)-4-(2-(4-chloro phenol) hydrazono) -3-methyl-5-oxo-4,5-dihydro-1H-pyrazole-1-carbothioamide	$C_{11}H_{10}ClN_5OS$ 295.03
E		(E)-4-(2-(4-nitro phenol) hydrazono) -5-oxo-4,5-dihydro-1H-pyrazole-1-carbothioamide	$C_{11}H_{10}N_6O_3S$ 306.05

2.4.2. Potentiodynamic polarization (PP) technique

Polarization tests were done in a traditional three electrode cell (platinum electrode, a saturated calomel anode (SCE) and working electrode. The working electrode was from Al sheet implanted in epoxy resin with the surface area (1.0 cm^2). Before every test the electrode surface was pretreated as in the weight reduction tests. The potential of electrode was reached to steady potential after 30 min before starting the measurements.

2.4.3. Electrochemical impedance spectroscopy (EIS) technique

Impedance estimations were completed utilizing AC signs of 5 mV peak to peak amplitude. All EIS information was fitted to proper proportional circuit utilizing the Echem Analyst (Gamry) programmer. The results of EIS were tested and deduced by using of the equivalent circuit.

The (% IE) and (θ) of the investigated PYRAZOLOCARBOTHIOAMIDE DERIVATIVES from the impedance tests can be computed from eq. (2) [10]:

% IE = θ x 100 = [1 – (R$^{\circ}_{ct}$ / R$_{ct}$)] x 100   (2)

Where R$^{\circ}_{ct}$ and R$_{ct}$ are the charge transfer resistances without and with inhibitor, individually

2.4.4-Electrochemical frequency modulation (EFM) tests

EFM tests carried out with relating perturbation signal with amplitude 10 mV with two sine waves of 2 and 5 Hz [11]. The larger peaks were utilized to calculate (i$_{corr}$) current from corrosion, Tafel constants (β_c and β_a) and (CF-2 and CF-3) causality factors [12]. Every electrochemical analysis was completed at 25±1°C, utilizing Gamry apparatus PCI300/4 Galvanostat/Potentiostat/Zra analyzer. DC105 corrosion software, EIS300 for EIS software, EFM140 for EFM software and Echem Analyst 5.5 for plotting, diagramming and information fitting and computing.

2.4.5. Surface examination

Surface analysis of Al pieces are soaked in several test solutions for a full day, isolated and dried. The shape of the surface of metal pieces was investigated by AFM technique. AFM technique roughness data from different surfaces is measured by AFM which act as a powerful technique. AFM is turning into an accepted method of roughness investigation [13]. AFM gave that immediate understanding into the adjustments in the surface shape take places at a few hundred nanometers when geographical changes because of the start of corrosion and preparation of forming film on the metal within the sight of inhibitors. AFM device model is a Pico SPM2100. Three and two measurement pictures were acquired from AFM device operating in contact mode in air at nanotechnology Laboratory, Faculty of Engineering Mansoura University. AFM pictures were scanned at 5µm × 5µm areas at a scan rate of 2.4 lines per second.

3. RESULTS AND DISCUSSION

3.1. Potentiodynamic polarization (PP) tests

Hypothetically, Al can corrode hardly in the deoxygenated corrosive arrangements [14]. In addition to, the PP diagrams show no steep slope in the anodic area, suggesting that no passive coating are formed on the surface of Al. PP were occurred in ability to accept information concerning the anodic and cathodic kinetics reactions. Figure 1 shows the PP performance of Al electrode with and without various concentrations of pyrazolocarbothioamide derivatives (A). The same diagrams obtained for other pyrazolocarbothioamide derivatives compounds (not shown). The data of PP parameters such as (i_{corr}), (E_{corr}), (β_c), (β_a), (θ) and (% IE) were measured from the curves of Figure 1 and are listed in Table 2 for all pyrazolocarbothioamide derivatives compounds. The data from Table 2 showed that both anodic and cathodic curves influenced by the presence of pyrazolocarbothioamide derivatives and the IE rises as the inhibitor concentration raised, suggesting that the presence of pyrazolocarbothioamide derivatives lower the anodic dissolution of Al and additionally impedes the cathodic reactions. In the existence of inhibitors, E_{corr} slightly changed, indicating that these compounds act as mixed–kind inhibitors in acidic medium creating an adsorbed layer at the Al/ solution interface. i_{corr} was lowered noticeably after the presence of inhibitors in HCl 2M and % IE improves with improving the inhibitor concentration. % IE and the level of (θ) were measured from eq. (3):

$$\% \text{ IE} = 100 \times \theta = 100 \times [(i_{corr} - i_{corr(inh)}) / i_{corr}] \tag{3}$$

Where i_{corr} and $i_{corr(inh)}$ are the unprotected and protected corrosion current densities data, correspondingly. Other words, the adsorbed pyrazolocarbothioamide derivatives lower the surface area available for anodic dissolution and hydrogen liberated at cathodic area without influencing the mechanism of reaction. The request of IE of the investigated compounds was observed to be: A > B > C > D > E.
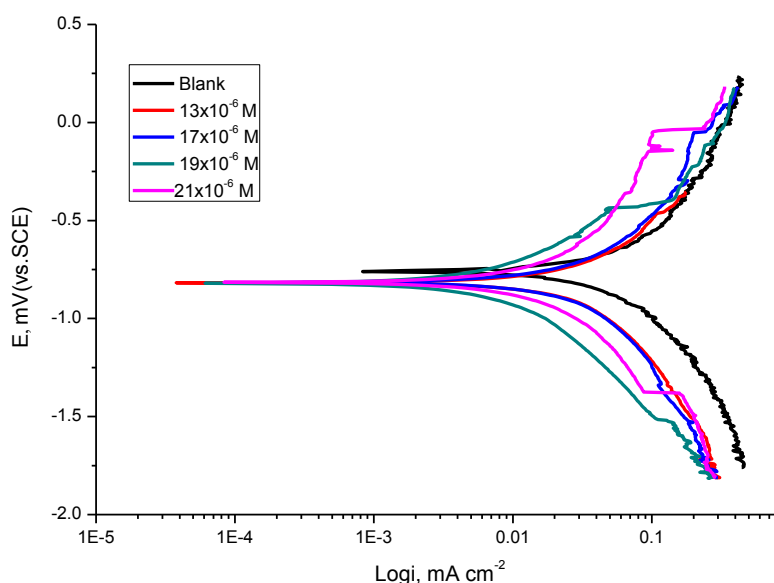

Figure 1. PP diagrams for the Al corrosion without and with different concentrations of inhibitor (A) at 25°C

Table 2. Data from PP of Al in 2M HCl contains different concentrations of investigated compounds at 25°C

Comp	Conc., x10^6 M 10^6 M	- E$_{corr,}$ mV vs SCE (vs SCE)	i$_{corr,}$ µA cm^{-2}	β$_c$ mV dec^{-1}	β$_a$ mV dec^{-1}	C.R x10^{-3} mpy	Ө	% IE
Blank	0.0	759.0	1095	431	346		-----	----
A	13	815.0	62.6	364	89	36.3	0.942	94.2
	17	815.0	60.3	364	89	35.1	0.944	94.4
	19	817.0	44.9	273	96	27.4	0.958	95.8
	21	815.0	24.9	255	89	17.4	0.977	97.7
B	13	816.0	75.5	251	96	42.7	0.930	93.0
	17	828.0	69.6	210	104	39.8	0.936	93.6
	19	806.0	43.4	252	117	26.7	0.960	96.0
	21	816.0	28.2	345	90.	19.1	0.974	97.4
C	13	830.0	89.2	287	95	49.6	0.918	91.8
	17	832.0	78.4	256	91	44.2	0.928	92.8
	19	829.0	46.4	233	97	28.2	0.957	95.7
	21	831.0	33.8	295	70	21.9	0.968	96.8
D	13	816.0	149	272	118	79.5	0.863	86.3
	17	830.0	90.6	269	116	50.3	0.916	91.6
	19	823.0	54.5	286	99	47.2	0.949	94.9
	21	824.0	76.8	270	88	43.4	0.929	92.9
E	13	825.0	457	323	82	233.5	0.580	58.0
	17	830.0	400	343	92	205	0.633	63.3
	19	832.0	305	368	88	157.5	0.720	72.0
	21	839.0	222	374	73	116.1	0.796	79.6

3.2. Electrochemical impedance spectroscopy (EIS) tests

Figure 2 displays the Nyquist diagrams get for the Al electrode at individual corrosion potentials after 30 min inundation in 2M HCl with and without various concentrations of pyrazolocarbothioamide derivatives (A) at 25°C. The same diagrams acquired for other compounds (not shown). As the inhibitor concentration rise, the semi-circle diameter rises. The deviation from ideal semicircle usually fit to the frequency dispersion as well as to the inhomogeneities of the Al surface [15]. EIS data of the pyrazolocarbothioamide derivatives were fitted utilizing the corresponding circuit, Figure 3, which signifies a single charge transfer reaction and fits well with our experimental obtained data [16]. C$_{dl}$ (double layer capacitance), for circuits contain a CPE parameter (Y^0 and n) were measured from eq. (4) [17]:

$$C_{dl} = Y^0 \omega^{n-1} / \sin[n(\pi/2)] \qquad (4)$$

$\omega = 2\pi f_{max}$, f_{max} = is the maximal frequency and n, is a customizable parameter that as a rule lies in the vicinity of 0.5 and 1.0. The diameter of half-circle calculated the resistance charge transfer, R$_{ct}$. An increase in R$_{ct}$ refers to rise in the width of the double layer that adsorbed by pyrazolocarbothioamide derivatives[18]. The data of (C$_{dl}$) lower by containing pyrazolocarbothioamide derivatives inhibitors into corrosive medium. Furthermore, C$_{dl}$ can be measure with the following equation:

$C_{dl} = \varepsilon\varepsilon_o \, (A/\delta)$ (5)

Where ε is constant dielectric double-layer, ε_o is vacuum electrical permittivity and δ is double-layer width. For the most part, the break down in C_{dl} data is ascribing to the replacement of the water molecules adsorbed at Al surface by the molecules of pyrazolocarbothioamide derivatives, which increases the dielectric constant [19] of the medium, and this dielectric constant inversely proportional to C_{dl}. Also, the decrease in surface size which plays as a site for charging may be measured as another reason for lowering the C_{dl}. The electrochemical parameters were recorded in Table 3. The order of IE obtained from EIS calculations is as next: A> B > C > D > E.
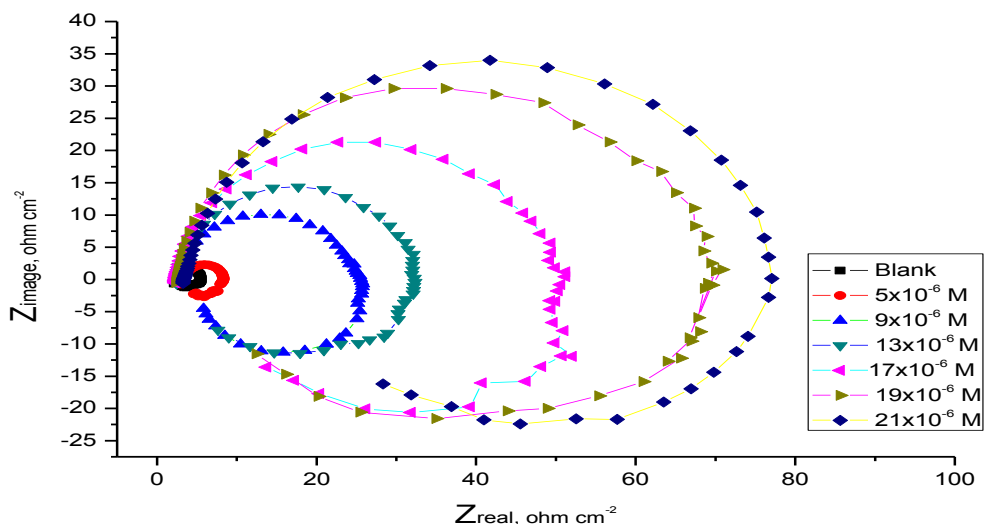
Figure 2. EIS Nyquist diagrams for Al in 2M HCl without and with various concentrations of pyrazolocarbothioamide derivatives (A) 25°C
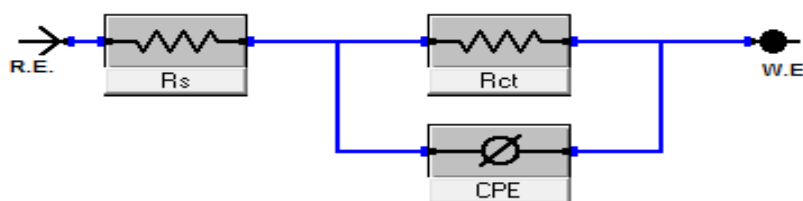
Figure 3. Corresponding circuit utilized to fit EIS values in 2M HCl solutions

Table 3. The obtained data of EIS test for Al without and with various concentrations of investigated compounds at 25°C

Comp	Conc., x 10^6 M	R_S, Ω cm^2	R_{ct}, Ω cm^2	C_{dl}, μFcm^{-2}	θ	%IE
Blank	0	3.5	1.07	121	----	----
A	5	2.8	3.90	9.10	0.724	72.4
	9	3.1	11.8	7.20	0.906	90.6
	13	2.7	19.4	5.10	0.945	94.5
	17	2.6	34.9	4.20	0.969	96.9

	19	3.0	39.1	3.80	0.972	97.2
	21	2.4	51.6	1.80	0.979	97.9
B	5	3.0	2.9	25.5	0.633	63.3
	9	2.9	7.9	15.7	0.864	86.4
	13	2.9	12.0	9.8	0.911	91.1
	17	2.3	18.9	8.5	0.943	94.3
	19	3.5	22.0	7.9	0.951	95.1
	21	3.2	34.7	7.1	0.969	96.9
C	5	2.7	2.4	34.5	0.561	56.1
	9	3.4	3.0	18.3	0.641	64.1
	13	2.9	3.9	15.0	0.724	72.4
	17	3.0	7.5	10.2	0.857	85.7
	19	2.3	12.0	8.3	0.878	87.8
	21	2.1	19.5	8.0	0.945	94.5
D	5	2.4	2.1	41.7	0.485	48.5
	9	2.4	2.2	19.6	0.514	51.4
	13	3.0	2.3	16.0	52.30	52.3
	17	2.2	2.5	11.8	0.563	56.3
	19	3.1	71.2	9.5	0.849	84.9
	21	2.5	9.1	8.3	0.881	88.1
E	5	2.8	1.1	50	0.050	5.0
	9	3.3	1.7	42.5	0.378	37.8
	13	2.2	2.2	28.2	0.514	51.4
	17	3.2	2.3	21.8	0.535	53.5
	19	2.9	2.4	16.5	0.564	56.4
	21	3.5	3.3	14.8	0.678	67.8

3.3. Electrochemical frequency modulation (EFM) tests

EFM is a nondestructive corrosion estimation method that can be straight and rapidly define the corrosion current data without earlier information of Tafel slopes, and with just a little PP sign. These aids of EFM procedure make it a perfect option for online corrosion detection [20]. The pronounced strength of the EFM is the (CF) causality factors that attend as an interior check on the power of EFM tests. The CF-2 and CF-3 are measured from the EFM spectrum of the present reactions. Figure 4 displays the EFM intermodulation spectra (current versus frequency) of Al in HCl solution containing various concentrations of compound (A). Similar intermodulation spectra were obtained for different compounds (not displayed). Every spectrum of EFM is a current reply as utility of frequency. The higher peaks were utilized to measure (i_{corr}), (β_c and β_a) and (CF-2 and CF-3). These EFM parameters were recorded in Table 5. The CF obtained under various test conditions are roughly equivalent to the hypothetical data (2 and 3) proving that the obtained data are confirmed and have best quality [12]. The %IE$_{EFM}$ increases by improving the pyrazolocarbothioamide derivatives concentrations and was calculated as in eq. (3). The % IE were evaluated from this test is in the order A > B > C > D > E.

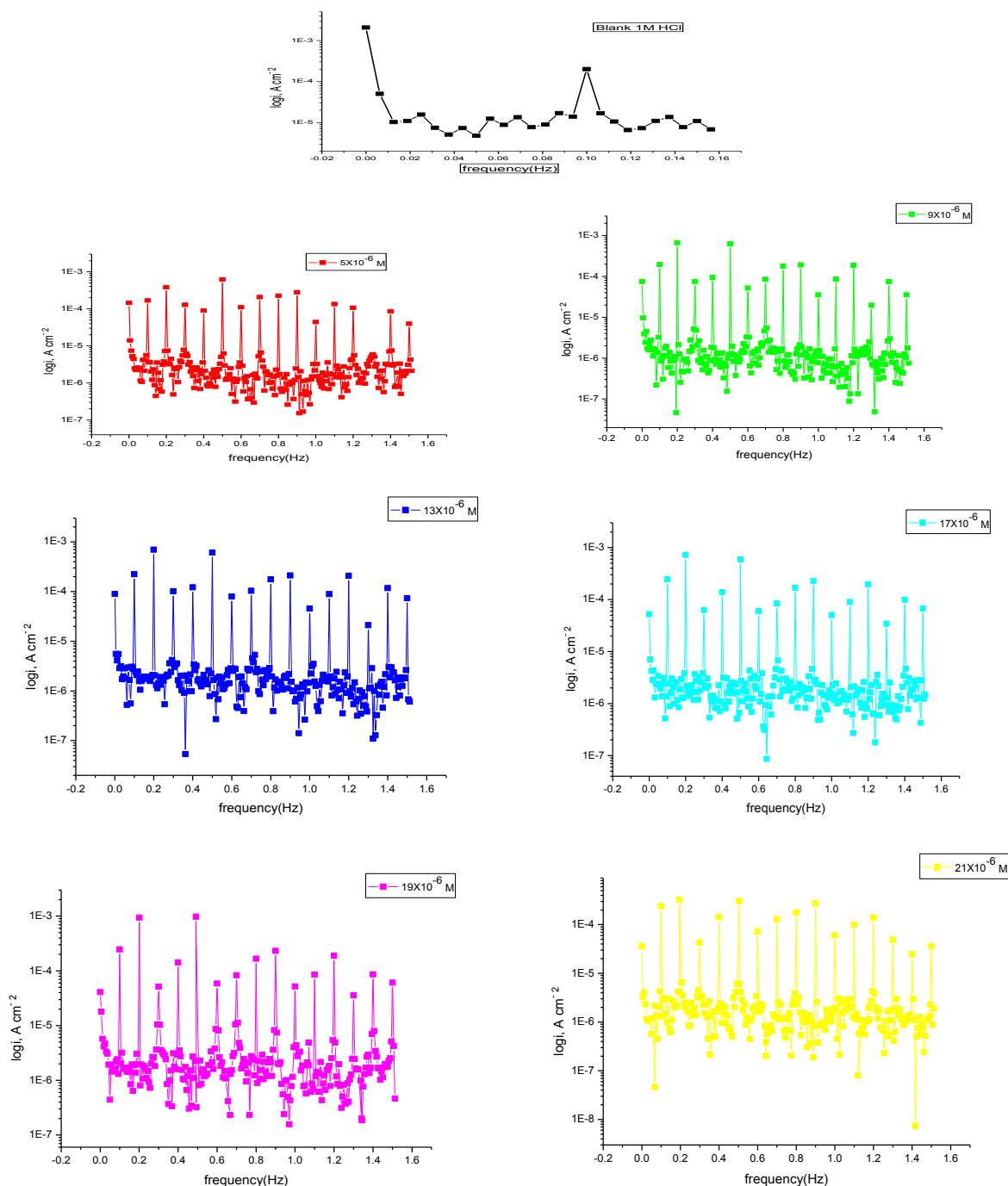**Figure 4.** EFM spectra for Al in 2 M HCl without and with various concentrations of compound (A)

Table 4. EFM parameters for Al without and with various concentrations of investigated compounds in 2M HCl at 25°C

Comp	Conc., x 10^6 M	i_{corr} ,μAcm^{-2}	β_c , $mVdec^{-1}$	β_a , $mVdec^{-1}$	C.R , mpy	CF-2	CF-3	θ	%IE
Blank	0.0	997	90	231	520	2.4	3.2	------	-----
	5	231.4	38	56	159.2	2.6	3.6	0.767	76.7
	9	213.1	32	43	134.1	1.9	2.6	0.786	78.6
	13	205.6	29	35	128.7	1.3	3.3	0.793	79.3

A	17	197.9	33	36	120.0	2.0	2.0	0.801	80.1
	19	183.2	24	30	118.3	2.3	3.1	0.816	81.6
	21	170.0	26	34	115.0	1.9	3.6	0.829	82.9
B	5	400.1	190	210	231.0	1.0	2.6	0.598	59.8
	9	360.7	193	206	212.9	1.8	3.1	0.638	63.8
	13	345.9	90	112	202.2	1.2	1.9	0.653	65.3
	17	302.5	81	105	160.2	2.0	2.9	0.696	69.6
	19	244.3	74	95	145.0	2.2	3.4	0.754	75.4
	21	220.6	50	87	132.6	1.6	3.5	0.778	77.8
C	5	455.2	170	207	276.7	2.0	3.1	0.543	54.3
	9	421.6	166	198	230.3	2.2	2.4	0.577	57.7
	13	396.0	87	121	216.8	2.0	3.0	0.602	60.2
	17	350.9	96	113	200.1	2.5	3.0	0.648	64.8
	19	271.1	66	79	173.3	2.1	3.7	0.728	72.8
	21	243.6	70	82	155.5	1.7	2.9	0.755	75.5
D	5	572.0	155	240	360.5	1.8	3.0	0.426	42.6
	9	505.1	140	203	304.3	1.7	2.6	0.493	49.3
	13	430.0	121	240	272.0	2.4	3.6	0.568	56.8
	17	380.6	152	214	244.0	1.2	3.3	0.618	61.8
	19	311.9	170	196	221.4	2.0	3.4	0.687	68.7
	21	279.3	153	166	206.9	1.7	2.9	0.719	71.9
E	5	645.7	187	220	390.0	2.3	2.9	0.352	35.2
	9	545.5	183	186	324.0	2.0	2.8	0.452	452
	13	490.3	97	130	292.0	1.5	2.0	0.508	50.8
	17	433.9	77	119	233.0	2.3	3.0	0.564	56.4
	19	407.4	82	90	204.0	2.7	3.2	0.591	59.1
	21	356	91	118	210.0	2.0	3.8	0.642	64.2

3.4. Weight reduction (WR) tests

The WR of Al samples in 2 M HCl solution, with and without various concentrations of the examined derivatives, was found after immersion 3 hours of at 25 ±1°C. Figure 5 signifies this for pyrazolocarbothioamide derivatives compound (A) for example. Similar plots were obtained for other compounds (not shown). Getting values of %IE are given in Table 5 at various concentrations from the investigated compounds at 25°C. The results displayed that the presence of investigated compound lowered the WR (mg cm^{-2}) and the rate of corrosion (mg cm^{-2} min^{-1}). The (%IE) and the θ, of the investigated compounds for the corrosion of Al were measured from eq. (1) [21]. % IE occurred by these compounds decreases in the next order: A > B > C > D > E.
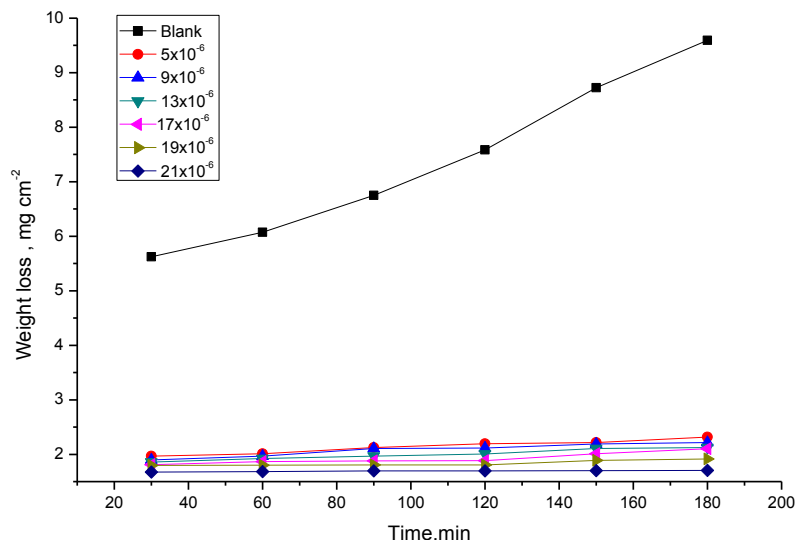
Figure 5. WR-Time diagrams for the dissolution of Al without and with various concentrations of compound (A) at $25^{\circ}C$

Table 5. % IE of all assembled at 120 min for Al in 2M HCl solution without and with various concentrations of investigated compounds as determined from WR technique at 25ºC

Comp.	A		B		C		D		E	
Conc., x 10^6 M	Θ	% IE	Θ	% IE	Θ	% IE	Θ	% IE	Θ	% IE
5	0.710	71.0	0.690	69.0	0.670	67.0	0.653	65.3	0.633	63.3
9	0.721	72.1	0.702	70.2	0.683	68.3	0.667	66.7	0.647	64.7
13	0.736	73.6	0.711	71.1	0.694	69.4	0.680	68.0	0.658	65.8
17	0.752	75.2	0.721	72.1	0.707	70.7	0.693	69.3	0.668	66.8
19	0.762	76.2	0.736	73.6	0.715	71.5	0.704	70.4	0.672	67.2
21	0.776	77.6	0.746	74.6	0.729	72.9	0.714	71.4	0.690	69.0

3.5. Influence of temperature

The influences of temperature on the protected acid-Al reaction is extremely complex, due to many exchanges happen on the Al surface, such as fast impression and desorption of the inhibitor and the inhibitor itself, the C.R. rise with the temperature improve. The temperature influence on the rate of corrosion of Al in 2 M HCl and in the presence of different inhibitor concentrations was studied in the range of temperature 298–318 K utilizing WR test. It was found that the IE decreases with raising temperature as displayed in Table 6, also the data from (Table 6) for compound (A) explains the adsorption decrease with increasing the temperature and corrosion rate (C.R.), similar tables were acquired for other compounds (not shown). Figure 6 variation of IE of compound (A) with various temperatures using different concentrations of compound (A) for Al corrosion in 2M HCl, (the same diagrams were acquired in existence of the other compounds, (but not presented). The decrease of % IE with temperature indicates that the inhibitors are adsorbed physical on the Al surface.
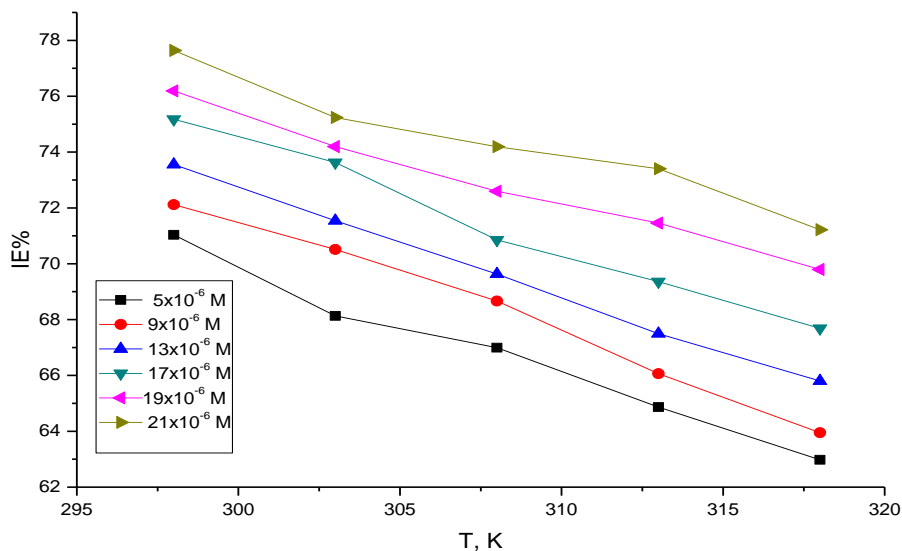
Figure 6. Effect of temperature on % IE at various concentrations of compound (A) for Al corrosion in 2M HCl with various temperatures

Table 6. Values of %IE, (θ) and corrosion rate (k_{corr}) for Al corrosion after 120 min immersion in 2M HCl in the absence and presence of various concentrations of compound (A) at various temperatures

Conc., x 10^6M	Temp, K	WR, mg cm^{-2}	k_{corr}, mg cm^2 min^{-1}	θ	%IE
blank		7.585	0.063	------	------
5		2.197	0.018	0.710	71.0
9		2.115	0.018	0.721	72.1
13		2.006	0.017	0.736	73.5
17	298	1.883	0.016	0.752	75.2
19		1.806	0.015	0.762	76.2
21		1.696	0.014	0.776	77.6
blank		10.5600	0.088	----	-----
5		3.3650	0.028	0.688	68.8
9	303	3.1140	0.026	0.705	70.5
13		3.0050	0.025	0.715	71.5
17		2.7850	0.023	0.736	73.6
19		2.7250	0.023	0.742	74.2
21		2.6150	0.022	0.752	75.2
blank		15.5300	0.129	-----	------
5		5.1260	0.043	0.670	67.0
9		4.8660	0.041	0.687	68.67
13	308	4.7160	0.039	0.696	69.6
17		4.5260	0.038	0.709	70.9
19		4.2560	0.035	0.726	72.6
21		4.0080	0.033	0.742	74.2
blank		19.2300	0.160	------	------

5		6.7560	0.056	0.648	64.8
9		6.5260	0.054	0.661	66.1
13	313	6.2510	0.052	0.675	67.5
17		5.8920	0.049	0.694	69.4
19		5.4890	0.046	0.715	71.5
21		5.1150	0.043	0.734	73.4
blank		27.6500	0.230		
5		10.2360	0.085	0.630	63.0
9		9.9680	0.083	0.640	64.0
13	318	9.4560	0.079	0.658	65.8
17		8.9350	0.074	0.767	67.7
19		8.3520	0.070	0.698	69.8
21		7.9580	0.066	0.712	71.2

The activation energy (E_a^*) of corrosion, procedure was measured utilizing Arrhenius eq. (6) [22]:

$$k_{corr} = A \exp(-E_a^* / RT) \qquad (6)$$

Where k_{corr} is rate of corrosion and A is Arrhenius constant. The data of E_a^* can be obtained from the slope lines of diagrams log k_{corr} vs 1/T (Fig.7) with and without examined compounds at various temperatures are recorded in Table 7. The increase in E_a^* with the presence of various concentrations of examined compounds display that the energy barrier for the corrosion reaction increases. These obtained data display that the presence of these inhibitors rise the E_a^* of the metal dissolution reaction ($E_a^* > 40$ kJ mol^{-1}). The activation in the hindering of the active center must be related with rise in the E_a^* of Al corrosion in the protected state [23-24]. ΔH^*, ΔS^* of activation are measured from transition state theory utilized the eq. (7) [25]:

$$k_{corr} = RT/Nh \exp(\Delta S^*/R) \exp(-\Delta H^* / RT) \qquad (7)$$

Figure 8 display diagrams of log (k_{corr}/T) vs. (1/T). Straight lines are obtained with a slope equal ($\Delta H^*/2.303$ R) and an intercept equal (log R/Nh + $\Delta S^*/2.303$ R), the data of ΔH^* and ΔS^* are recorded in Table 7. Usually, the enthalpy of a chemisorption procedure approaches (100 kJ mol^{-1}) [26-27]. The rise in the (ΔH^*) in presence of the pyrazolocarbothioamide derivatives means that the addition of these derivatives to 2M HCl solution rise the energy barrier of the corrosion reaction to an maximum degree rely on the concentration of pyrazolocarbothioamide derivatives. The values of ΔS^* are negative; this show that the activated complex in the rate-determining step represent association rather than dissociation step [28].
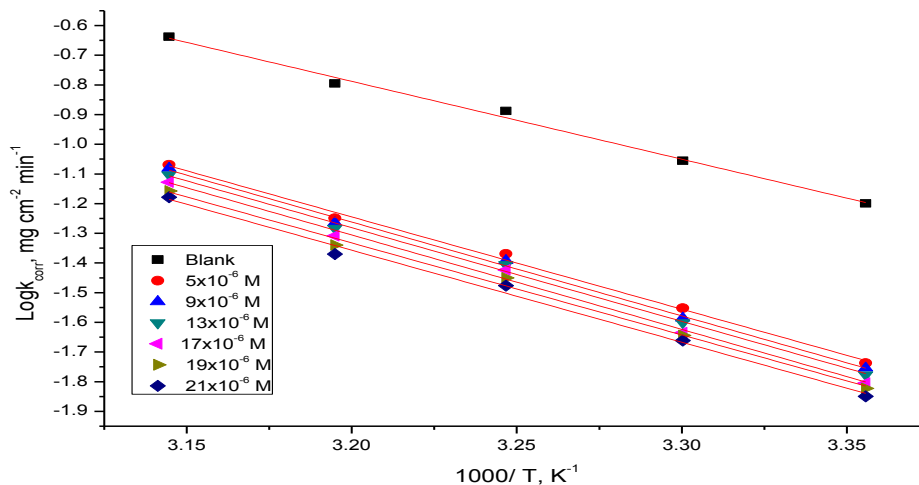
Figure 7. Arrhenius plots of variation for the dissolution of Al in 2.0 M HCl with and without various concentrations of compound (A)
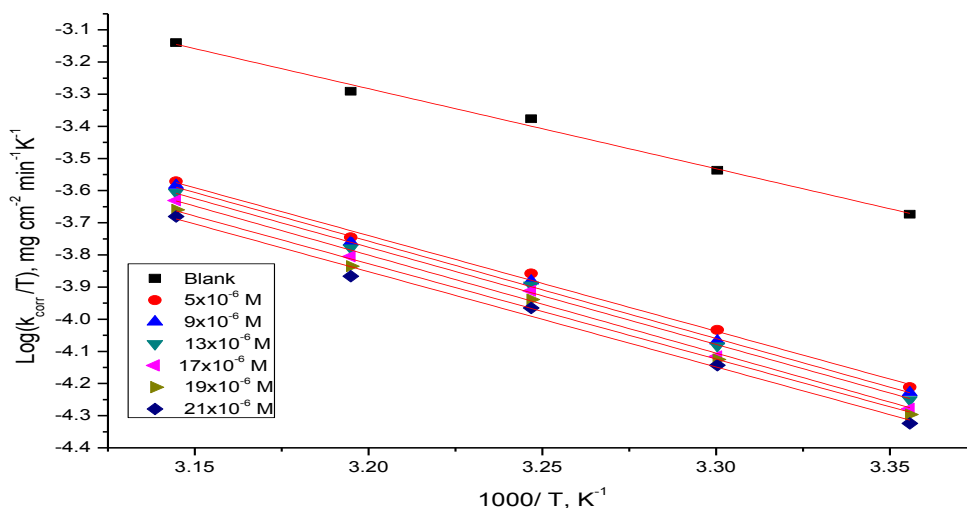

Figure 8. Plots of (log k_{corr} / T) vs. 1/ T for the dissolution of Al in 2M HCl with and without various concentrations of compound (A)

Table 7. Parameters for Al in 2 M HCl with and without various concentrations of investigated compounds

Comp	Conc., x 10^6 M	E_a^*, kJ mol^{-1}	$-\Delta H^*$, kJ mol^{-1}	$-\Delta S^*$, J mol^{-1}K^{-1}
Blank	0.0	50.2	47.6	107.8
A	5	59.5	56.9	92.6
	9	60.5	57.4	87.8
	13	60.4	57.8	84.6
	17	60.9	58.3	83.5
	19	61.2	60.9	83.7
	21	63.1	61.0	83.3
B	5	57.0	53.4	96.1
	9	59.5	55.4	92.6
	13	59.8	56.3	90.9

	17	60.2	57.2	90.8
	19	60.3	59.4	90.1
	21	61.1	60.1	86.4
C	5	56.4	52.9	98.0
	9	57.5	53.0	95.1
	13	58.1	54.4	92.9
	17	59.4	55.8	91.8
	19	59.8	56.3	90.9
	21	60.8	57.2	88.5
D	5	55.4	51.4	98.0
	9	56.5	51.8	96.6
	13	57.1	52.4	95.7
	17	59.0	54.4	95.0
	19	59.2	55.1	93.5
	21	60.1	55.5	92.2
E	5	53.0	50.6	100.3
	9	54.4	50.9	99.2
	13	56.1	51.4	97.0
	17	58.4	53.0	96.4
	19	59.0	55.0	94.0
	21	59.6	55.2	92.9

3.7. Adsorption isotherms

The essential data on the interface among the pyrazolocarbothioamide derivatives and the metal surface given by the adsorption isotherm and the sort of the inhibitors on metal is impacted by (i) the kind and charge of the Al (ii) compound structure of the pyrazolocarbothioamide derivatives and (iii) the kind of electrolyte [29-30]. Attempts were made to fit (θ) data to different adsorption isotherms. It is clear that the adsorption of inhibitors on the Al surface take after kinetic-thermodynamic model isotherm [31]. As can be found in Figure 9, the kinetic-thermodynamic model isotherm is the best one, which describes the test outcome results. The test information give good curves fitting for the applied adsorption isotherm as the relationship coefficients (R^2) near unit which were in the range (0.750-0.919). By that the kinetic-thermodynamic model of El-Awady et al [32] is valid to work the existing adsorption information eq. (8):

$$\text{Log} (\theta / (1-\theta)) = \text{Log } K' + y \text{ Log } C \tag{8}$$

Where θ is ($\theta = \%\ IE/100$), K_{ads} is the adsorption equilibrium constant, and the adsorption equilibrium constant $K_{ads} = K' (1/y)$, where $1/y$ is the number of active center for surface engaged by one inhibitors molecule. Figure 9 represents the plot of Log ($\theta / (1-\theta)$) against log C for compound (A) at different temperatures as an example. The same diagrams attained for other pyrazolocarbothioamide derivatives (not presented). Table 8 shows the effect of temperature on adsorption of the investigated compounds; the values of $1/y$, K_{ads} and ΔG^o_{ads} are calculated. In order to get a comparative view as shown in Fig 10, using kinetic-thermodynamic model for the adsorption of different concentrations of investigated compounds at 25ºC, the deviation of the (K_{ads}) of the pyrazolocarbothioamide derivatives with their molar concentrations was measured conferring to eq. (8). The values obtained of "**1/y**", K_{ads}

and ΔG°_{ads} are given in Table 8. The (K_{ads}) of adsorption, in eq. (9) could be further used to define free energy of adsorption (ΔG^o_{ads}) as follows**:**

$$\Delta G^o_{ads} = - RT \ln (55.5 \ K_{ads}) \qquad (9)$$

Where 55.5 is molar concentration (mol L^{-1}). The ΔG^o_{ads} and K_{ads} data for investigated compounds are list in Table 8. Generally, values of ΔG^o_{ads} around -20 kJ mol^{-1} or lower are consistent with the electrostatic association among the charged molecules and the charged Al physisorption. The measured ΔG^o_{ads} data are lower than -20 kJ mol^{-1} demonstrate that the adsorption of the pyrazolocarbothioamide derivatives on Al surface in 2 M HCl solutions was typical of physisorption, the estimation of (1/y) is more than unity. This implies the obtained pyrazolocarbothioamide derivatives molecules will possess more than one active center. The estimations of K_{ads} were found to run parallel to the% IE (KA > KB > KC > KD > KE).

Thermodynamic parameters such as ΔH°_{ads} and ΔS°_{ads} were computed using Vant't Hoff equation [33, 34] eq.(10):

$$\ln K_{ads} = \frac{-\Delta H^\circ_{ads}}{RT} + const \qquad (10)$$

Figure 10 displays the diagrams of log K_{ads} vs 1/T which provides straight lines with slope (- ΔH°_{ads}/ 2.303R), ΔS°_{ads} can be obtained using eq. (11):

$$\Delta G^o_{ads} = \Delta H^o_{ads} - T \ \Delta S^o_{ads} \qquad (11)$$

The thermodynamic parameters data for the pyrazolocarbothioamide derivatives adsorption were compute at temperature 25- 45°C and were listed in Table 8, which can elucidate the corrosion hindrance mechanism [35], an exothermic adsorption procedure $(\Delta H^o_{ads} < 0)$ may be either physisorption or chemisorption or mixture of both procedures. As, the absolute data of ΔH^o_{ads} obtained in this paper was lesser than (100 kJ mol^{-1}), this revealing of physisorption [36]. From the recorded values show that the computed data of ΔG^o_{ads} are around 15 kJ mol^{-1} and the e data of ΔH^o_{ads} obtained in this research was lesser than 40 kJ mol^{-1}, representative that the adsorption mechanism of examined compounds on Al in 2.0 M HCl solution at the research temperatures is of physisorption. Negative value ΔS^o_{ads} showed that decreasing in disorder of corrosion process on Al surface in 2 M HCl using pyrazolocarbothioamide derivatives as corrosion inhibitors (Table 8) [37-38].
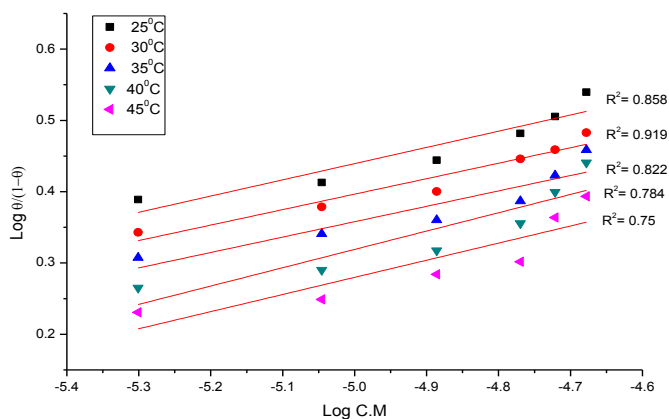

Figure 9. Adsorption isotherm curves from kinetic-thermodynamic model for the adsorption of compound (A) on Al in 2M HCl at various temperatures
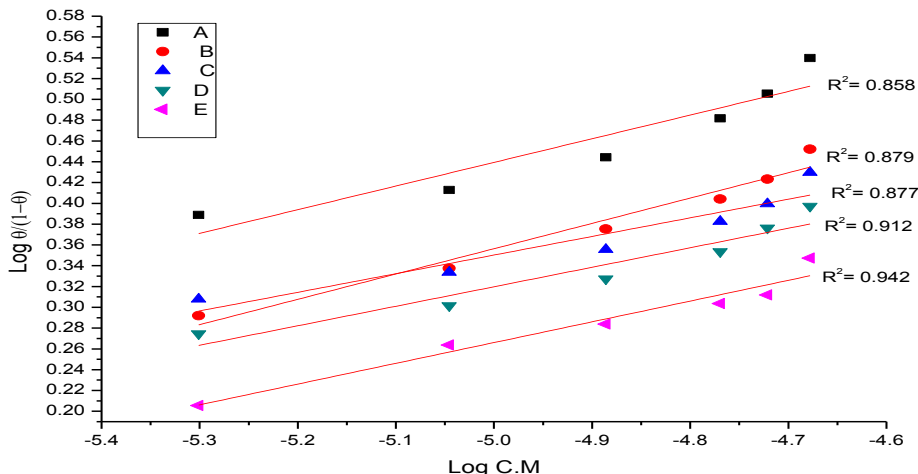
Figure 10. Adsorption isotherm curves from kinetic-thermodynamic model for the adsorption of various concentrations of investigated compounds at 25ºC
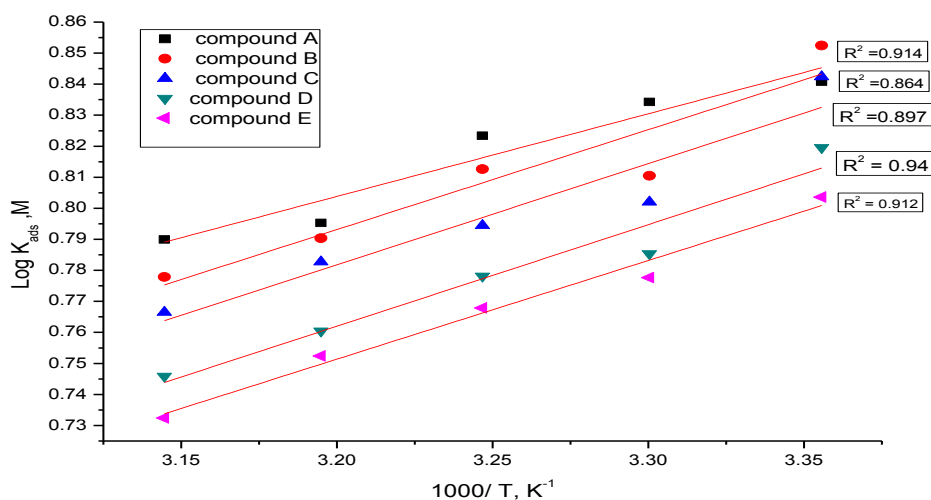

Figure 11. Van`t Hoff plots of variation of Log K_{ads} vs 1/T from kinetic-thermodynamic model for the adsorption of investigated pyrazolocarbothioamide derivatives in 2M HCl

Table 8. Thermodynamic parameters for Al 2M HCl for investigated compounds at various temperatures

Comp	Temp., K	K_{ads} M^{-1}	1/y	$-\Delta G^{\circ}_{ads}$ kJ mol^{-1}	$-\Delta H^{\circ}_{ads}$ kJ mol^{-1}	ΔS°_{ads} J mol^{-}K^{-1}
	298	7.5	4.4	14.9		49.4
	303	6.8	4.6	15.0		49.3
A	308	6.6	4.6	15.1	10.8	49.1
	313	6.2	3.8	15.2		48.5
	318	6.1	4.1	15.4		48.4
	298	7.1	5.4	14.8		49.6
	303	6.4	4.1	14.8		48.8
B	308	6.4	4.6	15.0	6.1	48.9
	313	6.1	4.1	15.2		48.5

	318	5.9	4.0	15.3		48.2
C	298	6.9	5.5	14.7	5.0	49.5
	303	6.3	4.5	14.8		48.7
	308	6.2	4.2	14.9		48.6
	313	6.0	4.8	15.1		48.4
	318	5.8	5.3	15.3		48.0
D	298	6.6	5.3	14.6	4.7	49.0
	303	6.1	4.2	14.7		48.4
	308	6.0	4.2	14.9		48.2
	313	5.7	3.9	15.0		47.9
	318	5.5	4.2	15.1		47.6
E	298	6.4	5.5	14.5	4.3	48.8
	303	6.0	4.5	14.6		48.2
	308	5.8	4.2	14.8		48.0
	313	5.7	4.8	15.0		47.9
	318	5.4	5.3	15.1		47.4

3.6. AFM analysis

AFM is a very important test for measuring the roughness of a sample surface at a maximum resolution in the order of fraction of nanometer [39]. AFM measurements are able to give details about the surface morphology of Al metal which is useful to corrosion science research. The three dimensional (3D) of AFM images appear as shown in Figure 12. Root Mean square roughness and average roughness The average roughness Ra can be defined as the average deviation of all points roughness profile that are measured from a mean line. Also, Root mean square roughness, Rq is the average deviation that are measured from the mean line.
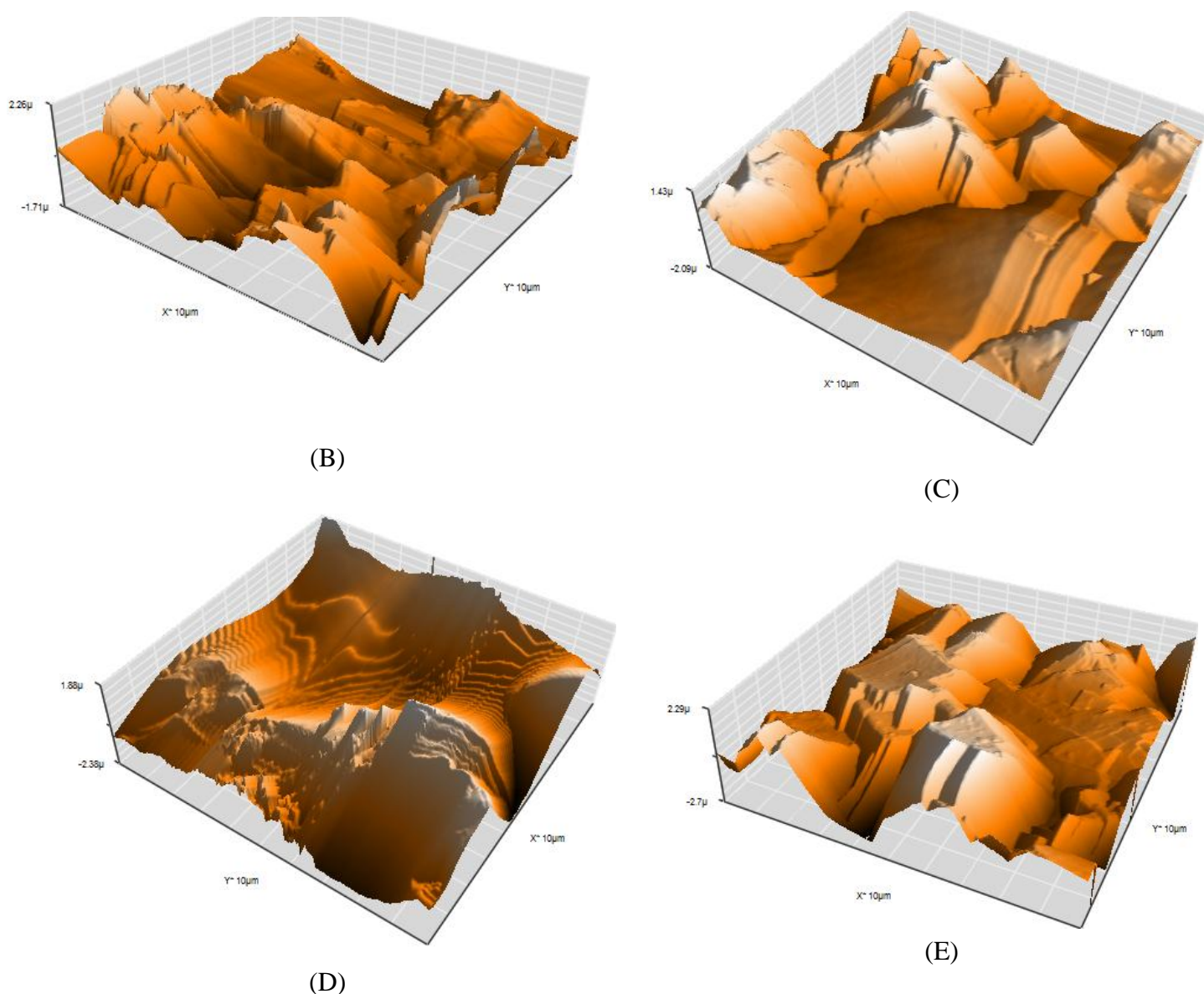

(Blank)

(A)

(B)

(C)

(D)

(E)
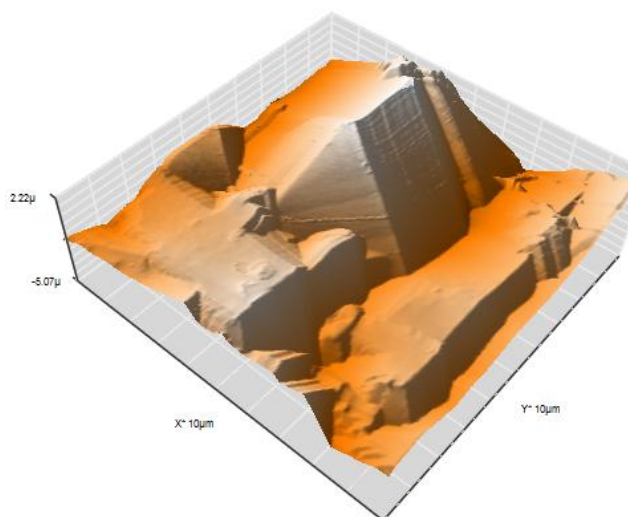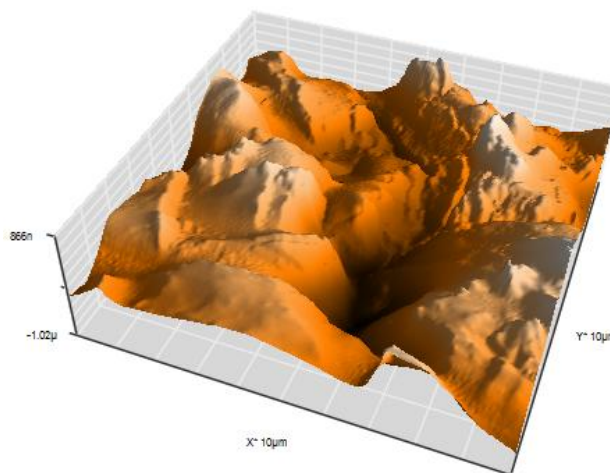
Figure 12. Three-dimensional (3D) AFM images Al metal before immersion in acid (free) Al metal immersed in 2M HCl alone (blank) and Al metal immersed in 2M HCl at 21×10^{-6} M of investigated compounds (A-E) for 24 hours at 25°C

Table 9. AFM roughness data of pyrazolocarbothioamide derivatives at 21×10^{-6}M for 24 hours at 25°C

Specimen	Average roughness(**Ra**) nm	RMS roughness (**Rq**) nm
Al metal surface (free)	45.33	53.96
Al metal immersed in 2M HCl (blank)	757.0	926.6
Al metal immersed in 2M HCl containing compounds (A)	246.1	309.3
Al metal immersed in 2M HCl containing compounds (B)	405.9	527.4
Al metal immersed in 2M HCl	449.3	567

containing compounds (C)		
Al metal immersed in 2M HCl containing compounds (D)	511	637
Al metal immersed in 2M HCl containing compounds (E)	864.4	678.4

The average roughness and root mean square roughness can be measured from AFM image. Ra is less sensitive than Rq to large and small high deviations from the mean .Table 9 gives the corresponding average roughness Ra and RMS roughness (Rq) values. A proportional view of the above roughness table clearly establishes that the surface of the metal is smoothened due to the adsorption coating formed due to active site in the inhibitors [40].

3.8. Chemical structure of inhibitors and corrosion protection

The corrosion hindrance of Al in 2 M HCl solution by some organic derivatives, using PP measurements, found to depend on concentration of the inhibitors, kind of metal, the mode of adsorption of the inhibitors and surface circumstances. These pyrazolocarbothioamide derivatives can be adsorbed in a flat orientation through the S, O and N atoms and the type of groups in para position. It was decided that the mode of adsorption rely on the empathy of the metal against the π-electron clouds of the ring system [41]. In addition to, the decrease in IE with rise in temperature, the order of decreasing the IE of the examined pyrazolocarbothioamide derivatives in 2 M HCl solution was: A > B > C > D > E. This performance can be rationalized basis of the structure-corrosion protection relationship of pyrazolocarbothioamide derivatives assembled. Linear free energy relationships (LFERs) have been used to correlate corrosion rate in the nonexistence and existence of the investigated compounds with their Hammett constituent constants (σ) giving indication for IE order. The LFER or Hammett relations [42] are given by:

$$\text{Log } (k_{\text{rate of corr}}/k^{o}_{\text{rate of corr}}) = -\rho\sigma \qquad (12)$$

Where k^{o} and are k the corrosion rates in the with and without of inhibitor, correspondingly. P is the reaction constant σ is the constituent in para-position, thus (ρ) is a qualified measure of the electron density at the reaction site. The constituent's σ which attract electrons from the reaction center (electron withdrawing groups) are dispersed positive data, but electron donating groups which have negative values. Plot of Log (rate) vs. σ and the slope is ρ and its signal designates whether the procedure is protect by improve or reduction of the electron density at the reaction site .The degree of ρ designates the relative sensitivity of the inhibition process to electronic effects. Figure13 displays that the examined assembles give a best correlation with correlation coefficient (R^2) (0.932). Assembled (A) has the maximum percentage hindrance efficiency, this being due to the attendance of p-OCH$_3$ group which is an electron donating group with negative Hammett constant ($\sigma_{pCH3} = -0.27$); this group will improve the density of electron charge on the molecule and may add an additional center of adsorption to the molecule. Assembled (B) comes after (A); this is due to the existence of *p*-CH$_3$ group which is an electron-donating group with Hammett constant ($\sigma_{CH3} = -0.17$), Also this group will rise the electron charge density on the molecule but with smaller amount than p-OCH$_3$group in

(A). Assembled (C) with Hammett constant ($\sigma_H = 0.0$) comes after (B) in %IE, due to H-atom in para position has no outcome on the charge density on the molecule. Lastly, compound (D) and compound (E) is the minimum in %IE. This is due to the attendance of p-Cl and p-NO_2 groups which being electron withdrawing group with positive Hammett constants ($\sigma_{Cl} = +0.23$ and $\sigma_{NO2} = +0.78$), rely on magnitude of their withdrawing character.
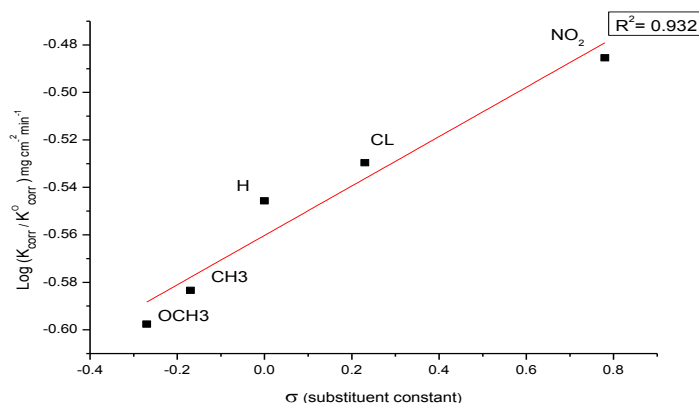

Figure 13. Relation between Log k_{corr} vs σ (Hammett constants) of the substituent of investigated compounds (A, B, C, D, E)

4. CONCLUSIONS

The Selected organic compounds acted as a corrosion inhibitors for Al in HCl 2M solution, the efficiency of these protected rely on their structures and the deviation in protective activity rely on the kind and the type of the substituent present in the pyrazolocarbothioamide derivatives molecules. The adsorptions of inhibitors rely on their concentrations, degree of temperatures and the natural of the inhibitor and metal. EIS results showed that improve in the R_{ct} and a lower in C_{dl} when the pyrazolocarbothioamide derivatives inhibitor is added and later improve in % IE. This is fit to rise of the thickness of the electrical double layer. PP results confirmed that the examined derivatives are mixed-kind inhibitors. The adsorption of all investigated organic compounds on Al surface obeys the kinetic-thermodynamic model isotherm and the type of adsorption is mixed adsorption. The presence of the protective film on the surface of Al was proving by AFM analysis. Chemical and electrochemical results were in excellent agreement.

References

1. V. Mountarlier, M.P. Gigandet, B. Normand, and J. Pagetti, *Corros. Sci.,* 47 (2005) 937.
2. P.G.Fox and P.A. Bradley, *Corros. Sci.*, 20 (1990) 643.
3. A. El Sayed, *J. Appl. Electrochem.*, 27 (1992) 193.
4. G. Schmitt, *Br. Corros. J.*, 19 (1984) 165.
5. M. Sykes, *Br. Corros. J.*, 25 (1990) 175.
6. P. Chatterjee, M. K. Banerjee and P. Mukherjee, *Ind. J. Technol.,* 29, (1991) 191.
7. M.M. Osman, E. Khamis, and A. Michael, *Corros. Prev. Control,* 41 (1994) 60.
8. S. Bilgic and N. Caliskan, J. Appl. Electrochem., 31 (2001) 79.
9. S. Bondock, H.El-Azap, E. M. Kandeel, M. A. Metwally, *Monatsh. Chem.*, 139 (2008) 1329

10. 10. H .Ma, S.Chen, L .Niu, S. Zhao, , S. Li, , D. Li, *J. Appl. Electrochem.*, .32(2002) 65.
11. R. W. Bosch, J. Hubrecht, W. F. Bogaerts, and B. C. Syrett, *Corrosion*, 57(2001) 60.
12. S. S. Abdel–Rehim, K. F. Khaled, N. S. Abd–Elshafi, *Electrochim. Acta*, 51 (2006) 3269.
13. Z. Khiati, A.A. Othman, M. Sanchez-Moreno, M. C. Bernard, S. Joiret, E.M.M Sutter, V. Vivier, *Corros. Sci.*, 35 (2011) 3092.
14. W.H. Smyrl, J.O.M. Bockris, B.E. Conway, E. Yeager, R.E. White (Eds.), Comprehensive Treatise of Electrochemistry, Plenum Press, New York, 4(1981) 116.
15. M. El Achouri, S. Kertit, H.M. Gouttaya, B. Nciri, Y. Bensouda, L. Pere, M. RInfante, K. Elkacemi, *Prog. Org. Coat.,* 43(2001) 267.
16. J.R. Macdonald, W.B. Johanson, J.R. Macdonald (Ed.), John Wiley& Sons, Fundamentals of impedance spectroscopy , book chapter 1, New York (1987) 1.
17. S. F. Mertens, C. Xhoffer, B. C. Decooman, E. Temmerman, *Corrosion,* 53 (1997) 381.
18. M. Lagrenée, B. Mernari, M. Bouanis, M. Traisnel, and F. Bentiss, *Corros. Sci.*, 44 (2002) 573.
19. F. Bentiss, M. Lagrenée, and M. Traisnel, *Corrosion,* 56 (2000)733.
20. E. Kus, F. Mansfeld, *Corros. Sci.*,48 (2006) 965.
21. D. Q. Zhang, Q. R. Cai, X. M. He, L. X. Gao, and G. S. Kim, *Mater. Chem. Phys.*, 114(2009) 612.
22. G. Trabanelli, in "Corrosion Mechanisms" (Ed. F. Mansfeld) Marcel Dekker, New York, (1987)119.
23. A.S. Fouda, A. Abd El-Aal, A.B. Kandil, *Desalination,* 201 (2006) 216.
24. F.H. Asaf, M. Abou- Krisha, M. Khodari, F. EL-Cheihk, A. A. Hussien, *Mater. Chem. Phys.*, 93 (2002) 1.
25. A. Fiala, A. Chibani, A. Darchen, A. Boulkamh, K. Djebbar, *Appl. Surf. Sci.*, 253(2007)9347.
26. S. T. Arab and E. A. Noor, *Corrosion,* 49(1993) 122.
27. W. Durnie, R.D. Marco, A. Jefferson, B. Kinsella, J. Electrochem. Soc., 146(1999) 1751.
28. M. K. Gomma and M. H. Wahdan; *Mater. Chem. Phys.* 39 (1995) 209.
29. E. Khamis, Corrosion, 46(1990)476.
30. A S Fouda, A.M. El-desoky, A.Nabih, *Advances in Materials and Corrosion*, 2 (2013)9.
31. A. N. Frumkin, *Zeitschrift für Physikalische Chemie,* 116 (1925) 466.
32. A. A. El-Awady,B. A. Abd El-Nabey and ,S. G. Aziz, *J. Electrochem. Soc.*, 139 (1992) 2149
33. L.Tang, X.Li, Y.Si, G.Mu and G.Liu, *Mater. Chem. Phys.*, 95 (2006) 29.
34. A. K.Maayta and N. A. F. Al-Rawashdeh, *Corros. Sci.*, 46 (2004)1129.
35. W. Durnie, R.D. Marco, A. Jefferson, B. And Kinsella, *J. Electrochem. Soc.*, 46 (1999)1751.
36. A. S. Fouda, D. Mekkiaand A. H. Badr, *J.Korean Chem. Soc.*, 57(2013) 264.
37. X. Li and G. Mu, *Appl. Surf. Sci.*, 252 (2005) 1254.
38. G.Mu, X. Li and G.Liu, *Corros. Sci.,* 47 (2005) 1932.
39. B. Wang, M. Du, J. Zang and C.J, Gao, *Corros.Sci.*, 53 (2011) 353.
40. S. Rajendran, C. Thangavelu and G. Annamalai, *J.Chem. Pharm. Res.,* 4 (2012) 4836.
41. L. R. Chauhan and G. Gunasekaran, *Corros. Sci.*, 49 (2007) 1143.
42. H. Ashassi-Sorkhabi, B. Shaabani, and D. Seifzadeh, *Appl. Surf. Sci.*, 239(2005)154.